Crystal Structure of Form I of Syndiotactic Poly(*para*-methylstyrene)†

Giuseppe Esposito, Oreste Tarallo, and Vittorio Petraccone*

Dipartimento di Chimica, Università di Napoli "Federico II", Complesso Monte S. Angelo, Via Cintia, I-80126 Napoli, Italy

Received April 28, 2006; Revised Manuscript Received May 26, 2006

ABSTRACT: The crystalline structure of form I of syndiotactic poly(*para*-methylstyrene) is described. In this form, the polymer chains assume a s(2/1)2 helical conformation and are packed according to the space group $P2_1/a$ in a unit cell with $a = 24.5$ Å, $b = 12.4$ Å, $c = 8.1$ Å, and $\gamma = 143.5°$. The proposed model may be described by a stacking of layers of alternating right- and left-handed helical chains efficiently packed in an "*interdigital structure*" in which phenyl rings belonging to one chain interlock with the phenyl rings of the two adjacent chains of opposite chirality. A disorder in the correct succession of the layers is suggested. A possible similarity between this form and the nanoporous δ form of syndiotactic polystyrene, suggested by the fact they are both obtainable by guest removal from α class clathrates, is analyzed.

Introduction

Highly syndiotactic poly(*para*-methylstyrene) (*s*-PPMS) is characterized by a very complex polymorphic behavior. In particular, it can crystallize in four different crystalline forms (I, II, III, and V), a mesomorphic one (form IV), as well as in several clathrate host−guest molecular complexes.[1−6] Moreover, the clathrate forms of *s*-PPMS described up to now can be divided in three different classes (α, β, and γ) differing in the conformation of the polymer chains assumed in the crystalline structure or in the way the chains are packed in the cell.[3,4] As far as the conformations of the polymorphic forms are concerned, forms III, IV, and V present a trans-planar conformation (with a repetition period of 5.1 Å)[2] while a s(2/1)2 chain conformation with a repetition period of 7.8 ± 0.1 Å has been found for forms I, II, and for α and β class clathrates.[2,7−10] In γ class clathrates, instead, polymer chains assume a $T_6G_2T_2G_2$ conformation with a repetition period of 11.7 ± 0.1 Å.[4] Up to now, only for the forms III[5] and IV[6] (both with trans-planar conformation), and for some clathrate structures belonging to α and β classes,[7−10] a complete structural characterization has been proposed, while the crystalline structures of forms I and II (both with s(2/1)2 helical conformation) have not been resolved yet. As far as the different types of clathrate forms of *s*-PPMS are concerned, in the framework of the present paper, it is worth pointing out that α class clathrates have been obtained with *o*-dichlorobenzene (*o*-DCB), *o*-xylene, *o*-chlorophenol, and *N*-methyl-2-pyrrolidone, which have very similar X-ray diffraction patterns.[3] On the basis of the crystal structure of the clathrate form containing *o*-DCB,[8] it can be said that these structures are characterized by centrosymmetric cavities (α class cavities) delimited by eight benzene rings belonging to two enantiomorphous adjacent helical chains. These kind of cavities are very similar to those present in all the crystal structure of the clathrate forms of syndiotactic polystyrene (*s*-PS), that for this reason have been classified as α class clathrates, too.[10]

In this paper, we present for the first time a complete structural characterization of form I of *s*-PPMS performed on the basis of structure factors and packing energy calculations. We were also motivated to investigate form I of *s*-PPMS from some experimental evidence suggesting a possible similarity between this crystalline form of *s*-PPMS and the nanoporous δ form of *s*-PS[11] for which some promising applications have been suggested due to its property to rapidly absorb low-molecular-weight molecules from different environments, even if present at low activity.[12−14] As a matter of fact, both of these two forms, which present chains in the same s(2/1)2 conformation with an identical periodicity, can be obtained removing guest molecules from the respective clathrate forms, both presenting α class cavities, by acetone treatments.[3,11] Therefore, in this paper, besides the structural model of *s*-PPMS form I, we present also a comparison between the packing evolution of *s*-PPMS and *s*-PS α class clathrate structures after the removal of guest molecules.

Experimental Section

s-PPMS was synthesized as described in ref 15. The syndiotacticity of the insoluble fraction in 2-butanone was evaluated by ^{13}C NMR analysis; the amount of the [*rrrr*] pentads was higher than 95%.

Unoriented form I samples can be obtained by crystallization from solution,[1] by thermal treatments of α class clathrates in the range 120−160 °C,[1,3] or by acetone treatments at room temperature of α class clathrates.[3] Crystallizations from solution produce samples of form I containing small amounts of form II, while the thermal treatments of α class clathrates produce form I samples with increasing amounts of form IV with rising of temperature. The unoriented sample of form I used in this paper, which does not contain any other crystalline form, was prepared by treatment of an unoriented clathrate sample containing *o*-DCB with acetone at room temperature. The unoriented clathrate sample containing *o*-DCB was prepared by casting at room temperature from 10 wt % *o*-DCB solution.

As far as oriented samples are concerned, these can be obtained only from oriented fibers of α class clathrate samples by annealing[2] or acetone treatments.[3] The acetone treatments produce samples characterized by a low degree of orientation, while the thermal treatments give rise to well-oriented samples, even if characterized by some amount of form IV.[2] However, because this mesomorphic form has a different periodicity (5.1 Å)[2] with respect to form I (8.1 Å), the only strong reflection that characterizes its diffraction pattern (placed on the first layer line) does not overlap with those of form I. For these reasons, oriented samples of form I were obtained by annealing oriented fibers of the clathrate form containing *o*-DCB for 2 h at 120 °C. The clathrate samples used were

† Dedicated to the memory of Professor Paolo Corradini.

* To whom correspondence should be addressed. E-mail: petraccone@chemistry.unina.it. Telephone: ++39 081 674309. Fax ++39 081 674090.

10.1021/ma060940p CCC: $33.50
Published on Web 06/30/2006

obtained by exposing the mesomorphic form IV to solvent vapors at room temperature, keeping fixed the ends of the specimens. Fibers of mesomorphic form IV have been prepared by drawing amorphous specimens at a temperature in the range of 115−120 °C, while amorphous samples have been obtained from melted samples quenched in ice−water.

Wide-angle X-ray diffraction patterns of unoriented samples were recorded by using an automatic Philips powder diffractometer (Ni-filtered Cu Kα radiation) operating in the $\theta/2\theta$ Bragg−Brentano geometry using specimen holders nearly 0.2 cm thick. The X-ray fiber diffraction patterns of oriented samples were obtained on a BAS-MS imaging plate (FUJIFILM) with a cylindrical camera (radius 57.3 mm, Ni-filtered Cu Kα radiation monochromatized with a graphite crystal) and processed with a digital scanner (FUJI-BAS 1800). Owing to the small number of reflections on the layer lines of the diffraction pattern obtained, the periodicity c has been determined collecting the 002 reflection with the same camera in tilted geometry by placing the fiber specimen with its axis normal to the cylindrical camera axis and oscillating it around the axis of the camera over an appropriate angular range.

Calculated structure factors were obtained as $F_c = (\sum |F_i|^2 M_i)^{1/2}$, where M_i is the multiplicity factor and the summation is taken over all reflections included in the 2θ range of the corresponding spot observed in the X-ray fiber diffraction pattern. A thermal factor ($B = 8$ Å^2) and atomic scattering factors from ref 16 were used. The observed structure factors F_o were evaluated from the intensities of the reflections observed in the X-ray fiber diffraction pattern (I_o) as $F_o = (I_o/Lp)^{1/2}$ where Lp is the Lorentz-polarization factor for X-ray fiber diffraction:

$$Lp = \frac{\left(\dfrac{0.5(\cos^2 2\theta + \cos^2 2\theta_M)}{1 + \cos^2 2\theta_M} + \dfrac{0.5(1 + \cos 2\theta_M + \cos^2 2\theta)}{1 + \cos 2\theta_M}\right)}{(\sin^2 2\theta - \zeta^2)^{1/2}}$$

with $2\theta_M = 26.6°$, the inclination angle of the monochromator, and $\zeta = \lambda(l/c)$, l and c being the order of the layer line and the chain axis periodicity, respectively, and λ the wavelength of the used radiation (1.5418 Å). The observed intensities I_o were evaluated integrating the whole area of the crystalline peaks observed in the X-ray diffraction profiles after the subtraction of the background (including the amorphous contribution) determined for each reflection by measuring the intensity in a region close to the reflection spot.

The discrepancy factor R has been evaluated as

$$R = \sum |F_o - F_c| / \sum F_o$$

taking into account only the observed reflections.

Energy calculations were carried out by using commercially available software (Cerius^2 version 4.2 by Accelrys Inc.) using the Compass[17] force field. The energy was minimized using the Open Force Field module by the smart minimizer method with standard convergence. The starting conformation of the *s*-PPMS polymer chains corresponds to that found by molecular mechanics calculations reported in the literature.[7]

Calculated X-ray powder diffraction patterns were obtained with the same software package using an isotropic thermal factor ($B = 8$ Å^2) and assuming the following dimensions for the crystallites: 120 Å along a and b axes and 80 Å along the c axis. In Figure 5, they are compared to the crystalline diffraction area obtained from the total area of the diffraction profile of an unoriented sample of *s*-PPMS in form I by subtracting the amorphous halo. The scattering of the amorphous phase has been obtained from the X-ray diffraction profiles of amorphous samples prepared by rapid cooling of the melt to room temperature.

Results and Discussion

The X-ray fiber diffraction pattern of an oriented sample of form I of *s*-PPMS is reported in Figure 1a. The diffraction pattern is poor of reflections showing only three reflections on the equatorial layer line, one on the first layer line, and two broad ones on the second layer line. This fact indicates a probably disordered crystalline structure. As usual for this kind of fiber diffraction pattern, owing to the not complete orientation of the crystallites in the fiber, a nearly meridional reflection, whose intensity is not evaluable, is also present. The positions and intensities of all the reflections observed in the diffraction pattern of Figure 1a are listed in Table 1. Table 1 also reports the positions of all the reflections observed in the powder diffraction pattern reported in Figure 1b of an unoriented sample. A good correspondence with the position of the reflections determined for the fiber is apparent.

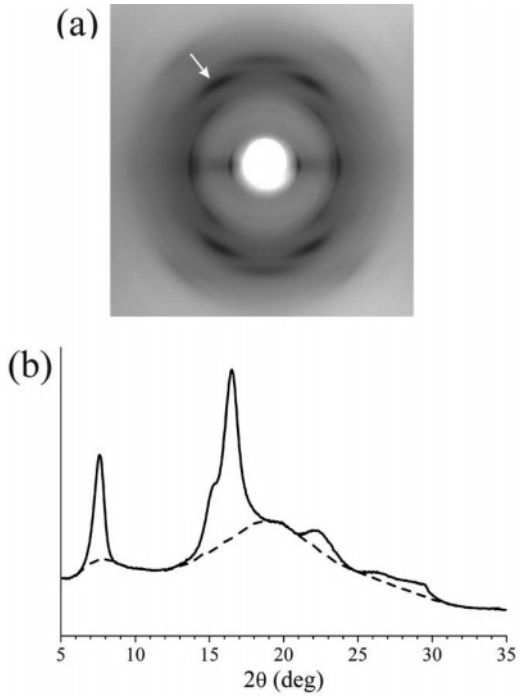

Figure 1. X-ray diffraction patterns of an oriented (a) and unoriented (b) sample in form I of s-PPMS. In (a), the presence of an amount of form IV is revealed by the reflections at $2\theta = 20.4°$ (indicated by the arrow), corresponding to the strongest reflections of that form.[2] Fiber axis is vertical. In (b), the dashed line indicates the contribution to the diffraction of the amorphous phase.

Table 1. Diffraction Angles ($2\theta_o$), Bragg Distances (d_o), and Intensities (I_o) in Arbitrary Units (AU) of the Reflections Observed on the Layer Lines (l) of the X-ray Fiber Diffraction Pattern of the Form I Specimen of s-PPMS Shown in Figure 1a.[a]

	X-ray fiber diffraction pattern			X-ray powder diffraction profile
l	$2\theta_o$ (deg)	d_o (Å)	I_o (AU)	$2\theta_o$ (deg)
0	7.6	11.63	4459	7.60
0	15.2	5.83	3610	15.35
0	16.3	5.44	9465	16.50
1	16.5	5.37	5275	
2	22.0[b]	4.04[b]	n.e.[c]	22.5 (broad)
2	26.8 (broad)	3.33	842	26.8 (broad)
2	28.6 (broad)	3.12	2201	28.7 (broad)

[a] Diffraction angles of the X-ray powder diffraction pattern of Figure 1b are also reported for comparison. [b] The $2\theta_o$ and d_o reported here corresponds to those read in the tilted geometry diffraction pattern. [c] The intensity of the nearly meridional reflection has not been evaluated (n.e.).

Determination of the Crystal Structure. The choice of a univocal unit cell only on the basis of a low number of observed reflections, as in this case, is rather problematic. To find a possible cell, we started from the hypothesis that this structure

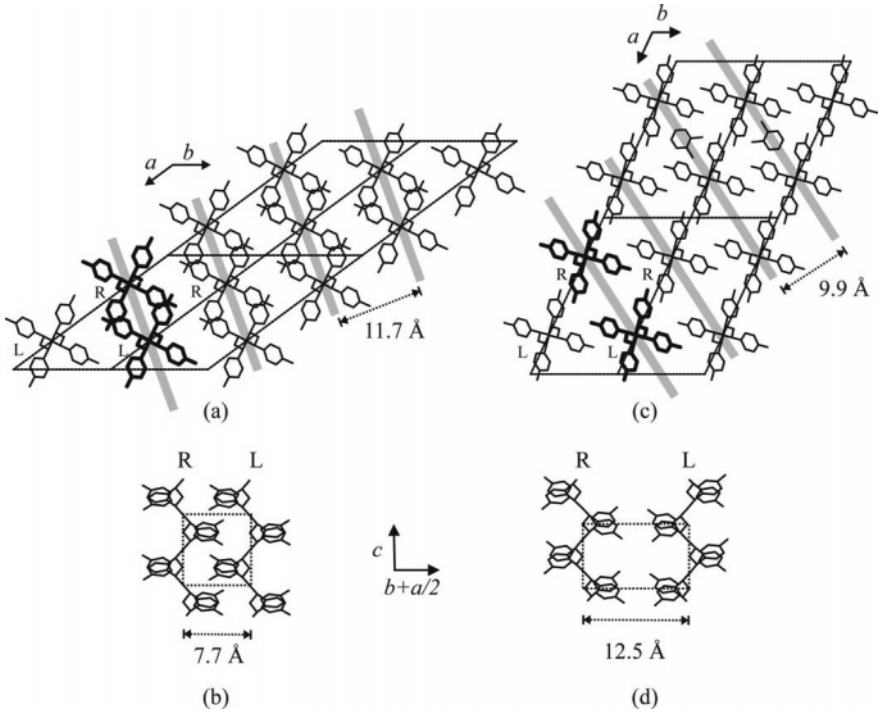

Figure 2. Comparison between the packing models proposed for the crystal structure of form I of s-PPMS (a, b) and for the crystal structure of the clathrate form of s-PPMS with *o*-DCB[8] (c, d), in the space group $P2_1/a$. In (a) and (c), the content of four unit cells is shown in the *ab* projection. In the upper cells of (c), two possible different arrangements of *o*-DCB molecules in the clathrate structure[8] are shown, while in the lower cells of (c) and in (d), only the "emptied" structure is shown. Gray stripes indicate the direction along which the polymer chains are supposed to approach to each other passing from clathrate to form I structure (see text for details). The distance between contiguous $c(b + a/2)$ polymer chain layers is also shown. In (b) and (d), the projection, perpendicular to the layers direction, of the packing between the couples of enantiomorphous polymer chains, drawn with bold lines in (a) and (c), are shown together with the distances among their chain axes. R = right-handed, L = left-handed helices.

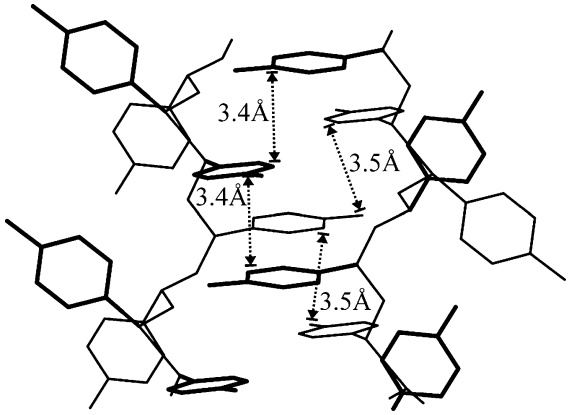

Figure 3. Projection of the two enantiomorphous helices represented in Figure 2b enlarged and rotated suitably with the aim of highlighting the interpenetration of the phenyl groups of the chains in the proposed structure. The closest nonbonded distances between sp^2 carbon atoms of interlocking phenyl groups, and those involving the methyl carbon atoms of a chain with the neighboring helix are indicated. Phenyl rings drawn with bold lines come toward the reader while those drawn with thin lines go away.

Table 2. Fractional Coordinates of the Atoms of an Asymmetric Unit of the Model Proposed (Figure 2a,b) for the Form I of s-PPMS[a]

	x/*a*	*y*/*b*	*z*/*c*
C1	0.248	−0.004	0.258
C2	0.211	−0.144	0.129
C3	0.171	−0.307	0.214
C4	0.221	−0.291	0.321
C5	0.184	−0.443	0.390
C6	0.095	−0.617	0.354
C7	0.044	−0.633	0.250
C8	0.081	−0.481	0.181
C9	0.285	−0.066	0.008
C10	0.056	−0.782	0.422
C11	0.177	−0.079	0.387
C12	0.094	−0.161	0.300
C13	0.100	−0.058	0.204
C14	0.023	−0.136	0.132
C15	−0.064	−0.319	0.151
C16	−0.069	−0.423	0.243
C17	0.008	−0.345	0.316
C18	−0.148	−0.403	0.079

[a] Hydrogen atoms were included in the structure factors calculation, but they are omitted in this table for simplicity

was strictly related to the crystal structure of α class clathrates, driven by the experimental observation that form I is obtainable from α class clathrates by acetone or thermal treatments (in particular, in ref 3 is shown that α class clathrates, after immersion in acetone at room temperature for few minutes, are transformed into form I, while in ref 18, electron diffraction experiments point out that, by heating to 120 °C single crystals of the clathrate form of *s*-PPMS including *o*-DCB, transformation into form I occurs). In particular, we supposed that *s*-PPMS form I could preserve a relative disposition of the chains similar to that found for the clathrate form containing *o*-DCB,[8] provided that the couples of polymer chains delimiting the cavities should move closer until they reach a close packing. As discussed later, this approach turned out to be winning, and it brought us to indexing the experimental reflections in terms of a monoclinic cell with constants $a = 24.5$ Å, $b = 12.4$ Å, $c = 8.1$ Å, and $\gamma = 143.5°$. The suggested space group is $P2_1/a$, in agreement with the systematic absence of $hk0$ reflections with $h = 2n + 1$ and $00l$ reflections with $l = 2n + 1$. Assuming two polymer chains in the s(2/1)2 helical conformation included in the unit cell, the crystalline density is 1.06 g/cm^3, in reasonable

Table 3. Comparison between Observed Structure Factors (F_o), Evaluated from the Intensities Observed in the X-ray Fiber Diffraction Pattern Shown in Figure 1a, and Calculated Structure Factors ($F_{c\_ordered}$ for the Completely Ordered Model and $F_{c\_disordered}$ for a Partially Disordered One) for the Model of Packing of Figure 2a,b in the Space Group $P2_1/a$[a]

hkl	$2\theta_o$ (deg)	$2\theta_c$ (deg)	d_o (Å)	d_c (Å)	F_o[b]	$F_{c\_ordered}$		$F_{c\_disordered}$	
$\bar{2}10$	7.60	7.55	11.63	11.70	85	79		79	
$\bar{4}20$	15.20	15.14	5.83	5.85	109	93		93	
$\bar{2}20$	16.30	15.99	5.44	5.54	183	126	181	126	181
410		16.32		5.43		130		130	
210		23.04		3.86		49		49	
011	16.50	16.25	5.37	5.45	118	97	135	97	135
201		16.36		5.42		95		95	
$\bar{3}21$		18.05		4.91		42		30	
$\bar{5}21$		21.20		4.19		57		40	
$\bar{5}31$		24.22		3.66		60		42	
$\bar{4}31$		24.63		3.61		34		34	
$\bar{6}21$		24.99		3.56		40		40	
$\bar{7}31$		27.83		3.21		37		26	
121		31.42		2.85		37		26	
002	22.0[c]	22.0	4.04[c]	4.04	n.e.[d]	87		87	
$\bar{1}02$	n.e.[d]	22.79	n.e.[d]	3.90	n.e.[d]	46		32	
$\bar{2}12$	n.e.[d]	23.24	n.e.[d]	3.83	n.e.[d]	60		60	
$\bar{1}12$	n.e.[d]	23.38	n.e.[d]	3.80	n.e.[d]	66		46	
$\bar{3}22$	26.80	26.31	3.33	3.39	52	73	94	51	78
$\bar{4}22$		26.77		3.33		59		59	
$\bar{5}22$	28.60	28.60	3.12	3.12	92	103	104	72	73
302		28.70		3.11		14		10	
$\bar{5}32$		30.95		2.89		55		39	
$\bar{4}32$		31.27		2.86		49		49	
$\bar{6}22$		31.57		2.83		66		66	
$\bar{6}32$		31.85		2.81		37		37	

[a] Bragg distances, observed in the X-ray fiber diffraction pattern and calculated for the proposed monoclinic unit cell ($a = 24.5$ Å, $b = 12.4$ Å, $c = 8.1$ Å, and $\gamma = 143.5°$), are also shown. Reflections not observed with F_c less than 30 have not been reported. [b] The reported F_o have been scaled in order to compare with $F_{c\_disordered}$. [c] The $2\theta_o$ and d_o reported here correspond to those read in the tilted geometry diffraction pattern. [d] Not evaluable.

agreement with the experimental value determined for amorphous samples (1.02 g/cm^3).[7,19]

The resulting structural model, optimized through molecular mechanics calculations, is shown in Figures 2a,b and 3. The fractional coordinates of the atoms of the asymmetric unit in the model of Figure 2a,b for the space group $P2_1/a$ are listed in Table 2. The calculated structure factors ($F_{c\_ordered}$) are compared in Table 3 to the experimental structure factors (F_o) evaluated from the X-ray fiber diffraction pattern of Figure 1a. A good agreement is apparent; the discrepancy factor is $R = 15\%$ for all observed reflections.

Packing Analysis. The proposed model may be described by a stacking of layers of alternating right- and left-handed helical chains in the plane defined by the *c* axis and the ($b + a/2$) direction. Within each layer, polymer helices are efficiently packed through an "*interdigital structure*" in which phenyl rings belonging to one chain interlock with the phenyl rings of the two adjacent chains of opposite chirality (see Figures 2b and 3). This kind of packing generates Csp^2−Csp^2 and methyl−Csp^2 carbon atom nonbonded distances (between phenyl rings belonging to adjacent enantiomorphous helices) in the range 3.4−3.6 Å, as shown in Figure 3. These distances can be justified by taking into account the fact that the phenyl rings are arranged in parallel planes, similarly to what happens in graphite crystals. The interlocking of the phenyl rings is likely to be the cause for the slightly greater value of the *c* axis found for this form (8.1 Å) with respect to that usually found for the clathrate structures of the same polymer whose structure has been determined up to now (7.8 ± 0.1 Å). All the other distances between carbon atoms of the same layer are equal to or greater than 3.6 Å. Distances between atoms belonging to chains of different layers are greater than 3.7 Å.

Figure 2 shows also a comparison between the crystal structure proposed for the form I of *s*-PPMS (Figure 2a,b) and that for the α class clathrate form of this polymer containing *o*-DCB (Figure 2c,d).[8] As hypothesized in the precedent section within the discussion about the choice of the unit cell, the crystalline structure of form I is strictly related to the structure of the clathrate form with *o*-DCB.[8] Referring to Figure 2, it can be said that the crystal structure of form I could be obtained starting from the "emptied" clathrate form containing *o*-DCB through a closer approach of the polymer chains along the ($b + a/2$) direction (the distance between their chain axes passes from 12.5 to 7.7 Å), accompanied by a $c/2$ shift of alternating polymer chains along the *c* axis (so that the phenyl rings of a chain interlock with those of adjacent chains of opposite chirality). As a consequence, new short distances arise between lateral groups of chains belonging to different layers that are relaxed through the retreat of the layers revealed by an increase of the distance between them from 9.9 to 11.7 Å.

This behavior is different from that observed for the clathrates of *s*-PS. Also in those cases, acetone can be used as an emptying agent, but at variance with *s*-PPMS, those clathrate forms give rise to an emptied nanoporous form, the δ form, characterized by a crystal structure basically identical to that of the clathrate from which it has been obtained, in which α class cavities are still present even if with a smaller volume.[11] These cavities can host small guest molecules (like dichloroethane)[20] without modifying significantly the unit cell dimensions or bigger molecules (like *o*-DCB)[21] varying properly the cell parameters.[22] As a consequence, the crystalline density of the nanoporous δ form is 0.98 g/cm^3, noticeably lower than the density of amorphous samples (1.05 g/cm^3).[11] It is worth noting that, by annealing at temperatures higher than T_g of *s*-PS (≅100 °C), the δ form gives rise to the thermodynamically more stable γ form (experimental density 1.07 g/cm^3 for samples with a degree of crystallinity of nearly 45%).[23]

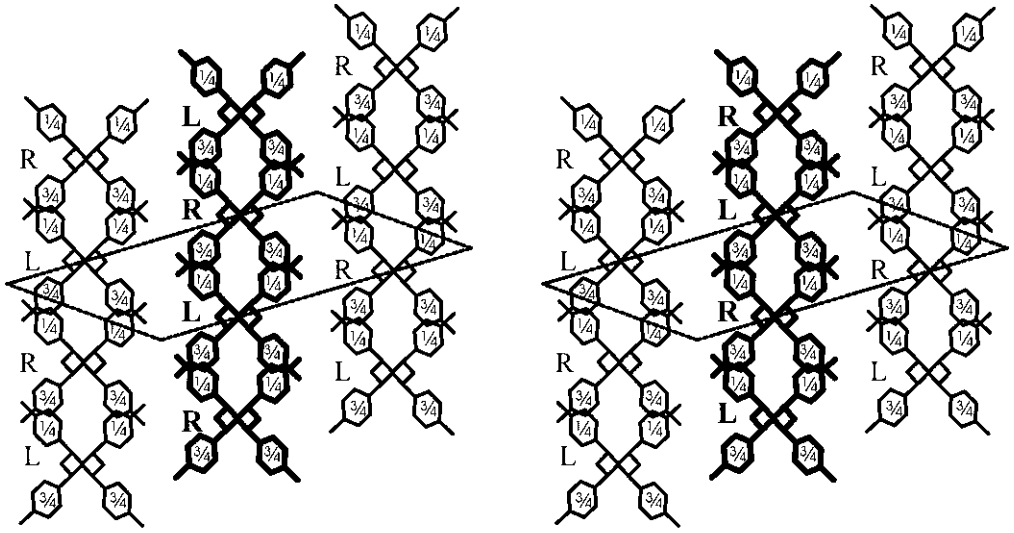

Figure 4. Possible disorder present in the proposed structure of the form I of s-PPMS. In (a), the completely ordered succession of $c(b + a/2)$ layers of chains is represented (see also Figure 2a) according to the $P2_1/a$ symmetry, while in (b), a possible fault is represented. R = right-handed, L = left-handed helices. The approximate fractional coordinates z/c of the barycenters of the phenyl rings are also shown.

Reasonably, this is a consequence of the fact that the crystal structure of the δ form represents a metastable structure, corresponding to a local relative minimum of energy, close to the structure of the *s*-PS clathrates deprived of the solvent from which they have been obtained (as indicated by the calculations reported by one of us in Table 3 of ref 11). Unluckily, this situation does not happen in the case of the α class clathrate forms of *s*-PPMS, for which the removal of the solvents brings directly a very efficient packing of the chains that were delimiting the cavities. Therefore, in the case of *s*-PPMS, an analogous "empty" form does not exist.

Possible Disorder. As apparent from Table 3, the suggested structural model for the form I of *s*-PPMS is characterized by a good agreement with the observed experimental data, but it produces also some calculated but not observed reflections slightly greater than the lowest observed one (see column $F_{c\_ordered}$). These calculated reflections are all on the layer lines and for 2θ greater than 20°. This fact leads us to suppose the presence of some kind of disorder in the structure, mainly related to the *z* coordinate of the atoms. A possible disorder compatible with this kind of layered structure is a random translation of $(a/2 + b)$ of each layer with respect to the others. An example of this kind of disorder is shown in Figure 4.

This kind of disorder is certainly compatible with the proposed crystal structure because, for the "ordered" and "disordered" structure, both the smallest nonbonded distances (3.7 Å) between atoms of polymer helices belonging to different layers and the packing energy remain basically unaltered. The expected consequence of this disorder is the lowering (until reaching zero for a complete statistical case) of the calculated intensity for layer line reflections *hkl* with $h = 2n + 1$. This fact is beneficial for the most of the calculated but not observed reflections discussed before, while the unique strong reflection observed on the first layer line (indexed as 011 + 201) would remain unaltered. At the same time, this fact would improve the agreement with the experimental data of the first reflection at $2\theta = 26.8°$ on the second layer line (see Table 3). The only "negative" consequence of the introduction of this kind of disorder would be a too low calculated F_c for the second observed reflection at $2\theta = 28.6°$ on the second layer line (see column $F_{c\_ordered}$ of Table 3). The best compromise, for which the lowest discrepancy factor *R* is obtained (= 13%), accompanied by a decrease of the calculated but not observed reflections *hkl* with $h = 2n + 1$, is the introduction of a partial disorder of 15% of the layers shifted with respect to the ordered structure (see column $F_{c\_disordered}$ of Table 3).

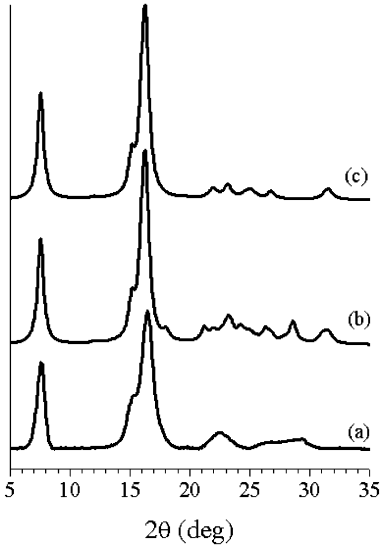

Figure 5. Comparison between experimental X-ray powder diffraction profile of the sample of s-PPMS form I, reported in Figure 1b, after the subtraction of the amorphous halo (curve a) and the diffraction profiles calculated for the ordered model of Figure 2a, b (curve b) and for the completely disordered one (curve c). See text for details.

An alternative representation of the effect of a possible disorder of this type on the diffraction pattern is given in Figure 5, where there are reported the experimental diffraction pattern (after the subtraction of the amorphous contribution) of the unoriented sample of form I (Figure 5a) of Figure 1b, the calculated one obtained from the proposed model (Figure 5b) and the calculated diffraction pattern corresponding to the limit disordered model in which each site is occupied at 50% by a right- and a left-handed polymer chain (Figure 5c).

Conclusions

The crystalline structure of form I of *s*-PPMS is described. The structure presents a monoclinic unit cell with $a = 24.5$ Å, $b = 12.4$ Å, $c = 8.1$ Å, and $\gamma = 143.5°$, in which ***s***(2/1)2 polymer chains are packed according to the space group $P2_1/a$. The proposed model may be described by a stacking of layers of alternating right- and left-handed helical chains. Within each layer, polymer helices are efficiently packed through an "*interdigital structure*" in which phenyl rings belonging to one chain interlock with the phenyl rings of the two adjacent chains of opposite chirality. The proposed structure seems strictly related to that of the α class clathrate forms in the sense that it could be obtained starting from the "emptied" α class clathrates through a closer approach of the polymer chains along the direction in which the cavities are formed until the phenyl rings of a chain interlock with those of adjacent chains of opposite chirality. The obtaining of this structure could explain why *s*-PPMS does not give rise to a nanoporous form as observed in the case of *s*-PS δ form.

Acknowledgment. Financial support of the "Ministero dell'Istruzione, dell'Università e della Ricerca" (PRIN2004 project) is gratefully acknowledged.

References and Notes

(1) Iuliano, M.; Guerra, G.; Petraccone, V.; Corradini, P.; Pellecchia, C. *New Polym. Mater.* **1992**, *3*, 133−144.
(2) De Rosa, C.; Petraccone, V.; Guerra, G.; Manfredi, C. *Polymer* **1996**, *37*, 5247−5253.
(3) Dell'Isola, A.; Floridi, G.; Rizzo, P.; Ruiz de Ballesteros, O.; Petraccone, V. *Macromol. Symp.* **1997**, *114*, 243−249.
(4) Petraccone, V.; Esposito, G.; Tarallo, O.; Caporaso. L. *Macromolecules* **2005**, *38*, 5668−5674.
(5) De Rosa, C.; Petraccone, V.; Dal Poggetto, F.; Guerra, G.; Pirozzi, B.; Di Lorenzo, M. L.; Corradini, P. *Macromolecules* **1995**, *28*, 5507−5511.
(6) Ruiz de Ballesteros, O.; Auriemma, F.; De Rosa, C.; Floridi, G.; Petraccone, V. *Polymer* **1998**, *39*, 3523−3528.
(7) Petraccone, V.; La Camera, D.; Pirozzi, B.; Rizzo, P.; De Rosa, C. *Macromolecules* **1998**, *31*, 5830−5836.
(8) Petraccone, V.; La Camera, D.; Caporaso, L.; De Rosa, C. *Macromolecules* **2000**, *33*, 2610−2615.
(9) La Camera, D.; Petraccone, V.; Artimagnella, S.; Ruiz de Ballesteros, O. *Macromolecules* **2001**, *34*, 7762−7766.
(10) Petraccone, V.; Tarallo, O. *Macromol. Symp.* **2004**, *213*, 385−394.
(11) De Rosa, C.; Guerra, G.; Petraccone, V.; Pirozzi, B. *Macromolecules* **1997**, *30*, 4147−4152.
(12) Guerra, G.; Milano, G.; Venditto, V.; Musto, P.; De Rosa, C.; Cavallo, L. *Chem. Mater.* **2000**, *12*, 363−368.
(13) Milano, G.; Venditto, V.; Guerra, G.; Cavallo, L., Ciambelli, P.; Sannino, D *Chem. Mater.* **2001**, *13*, 1506−1511.
(14) Mensitieri, G.; Venditto, V.; Guerra, G. *Sens. Actuators, B* **2003**, *92*, 255−261.
(15) Zambelli, A.; Longo, P.; Pellecchia, C.; Grassi, A. *Macromolecules* **1987**, *20*, 2035−2037.
(16) Cromer, D. T.; Mann, J. B. *Acta Crystallogr., Sect. A* **1968**, *24*, 321−324.
(17) Sun, H *J. Phys. Chem. B* **1998**, *102*, 7338−7364.
(18) Rizzo, P.; Ruiz de Ballesteros, O.; De Rosa, C.; Auriemma, F.; La Camera, D.; Petraccone, V.; Lotz, B. *Polymer* **2000**, *41*, 3745−3749.
(19) The crystalline density of form I is compared to the experimental one determined for completely amorphous samples obtained by compression molding and not with that determined for semicrystalline form I samples obtained through solution procedures because, in this latter case, the experimental density is misleadingly too low, even lower than that of amorphous samples. This fact can be justified in the hypothesis the amorphous phase of form I samples obtained in this way have a porous structure, as discussed in the case of clathrate samples of other syndiotactic polystyrenes (see note 23 in Petraccone, V.; Tarallo, O.; Califano, V. *Macromolecules* **2003**, *36*, 685−691).
(20) De Rosa, C.; Rizzo, P.; Ruiz de Ballesteros, O.; Petraccone, V.; Guerra, G. *Polymer* **1999**, *40*, 2103−2110.
(21) Tarallo, O.; Petraccone, V. *Macromol. Chem. Phys.* **2004**, *205*, 1351−1360.
(22) Tarallo, O.; Petraccone, V.; Venditto, V.; Guerra, G. *Polymer* **2006**, *47*, 2402−2410.
(23) Manfredi, C.; De Rosa, C.; Guerra, G.; Rapacciuolo, M.; Auriemma, F.; Corradini, P. *Macromol. Chem. Phys.* **1995**, *196*, 2795−2808.

MA060940P